

AD-A261 122



NTATION PAGE

Form Approved
OMB No. 0704-0188

2

ated to average 1 hour per response, including the time for reviewing instructions, searching existing data sources, reviewing the collection of information. Send comments regarding this burden estimate or any other aspect of this burden, to Washington Headquarters Services, Directorate for Information Operations and Reports, 1215 Jefferson Office of Management and Budget, Paperwork Reduction Project (0704-0188), Washington, DC 20503.

1. AGENCY USE ONLY (Leave blank)		2. REPORT DATE 17/18/93	3. REPORT TYPE AND DATES COVERED Technical	
4. TITLE AND SUBTITLE Passivity Motivated Controller Design for Flexible Structures			5. FUNDING NUMBERS DAAL03-92-G-0123	
6. AUTHOR(S) Declan Hughes and John T. Wen				
7. PERFORMING ORGANIZATION NAME(S) AND ADDRESS(ES) Rensselaer Polytechnic Institute Dept. of Civil & Env. Engineering, JEC 4049 110 - 8th Street Troy, NY 12180-3590			8. PERFORMING ORGANIZATION REPORT NUMBER	
9. SPONSORING/MONITORING AGENCY NAME(S) AND ADDRESS(ES) U. S. Army Research Office P. O. Box 12211 Research Triangle Park, NC 27709-2211			10. SPONSORING/MONITORING AGENCY REPORT NUMBER ARO 30378.1-E6-URI	
11. SUPPLEMENTARY NOTES The view, opinions and/or findings contained in this report are those of the author(s) and should not be construed as an official Department of the Army position, policy, or decision, unless so designated by other documentation.				
12a. DISTRIBUTION/AVAILABILITY STATEMENT Approved for public release; distribution unlimited.			12b. DISTRIBUTION CODE	
13. ABSTRACT (Maximum 200 words) When actuators and sensors on a controlled mechanical structure form naturally passive pairs, which usually requires physical collocation, very robust stabilizing controllers can be constructed. If the number of such naturally passive pairs is small, the closed loop performance may not be satisfactory. To address this problem, additional sensors, which are usually cheaper, lighter and easier to instrument than actuators, are frequently added to the control system. However, the passivity property no longer holds for these sensors with respect to the existing actuators. This paper presents some results on extending the passivity based design to incorporate these non-collocated sensors by using some nominal model information to synthesize a fictitious strictly passive output. The design approach was applied to a single rotating flexible beam with encouraging results.				
14. SUBJECT TERMS			15. NUMBER OF PAGES 12	
			16. PRICE CODE	
17. SECURITY CLASSIFICATION OF REPORT UNCLASSIFIED		18. SECURITY CLASSIFICATION OF THIS PAGE UNCLASSIFIED	19. SECURITY CLASSIFICATION OF ABSTRACT UNCLASSIFIED	20. LIMITATION OF ABSTRACT UL

NSN 7540-01-280-5500

Standard Form 298 (Rev 2-89)
Prescribed by ANSI Std. Z39-18
298-102

ation

☒ ☐

Department of Electrical, Computer, and Systems Engineering
Rensselaer Polytechnic Institute
Troy, NY 12180
518-276-8744 wen@ral.rpi.edu

Availability Codes	
Dist	Avail and/or Special
A-1	

A-1

Most of the published work on multiple articulated flexible bodies either deal with lumped joint flexibility or distributed link flexibility, seldom both. The most prominent theoretical approach to the control of systems containing lumped joint flexibility is based on the exact linearization method, for a summary see [4]. In general, this approach requires the exact model information, linear spring assumption, and zero gyroscopic force coupling. Furthermore, the feedforward compensation (for the exact linearization) and the feedback stabilization are intertwined and errors in the feedforward may affect the closed loop stability in an adverse way. In contrast, the passivity approach requires much less model information in the set point control case (only the spring and gravity models are needed), can be extended to a nonlinear spring and the fully coupled dynamic model, and the additive separation between the feedback and feedforward implies that error in feedforward does not lead to instability [5]. The price is that the closed loop performance cannot be arbitrarily assigned. Passivity property for structures with lumped flexibility (e.g., flexible joint robots) has

93-03271



25 P 8

been recognized in [6] and has been used in a proportional-derivative (PD) controller design. The method requires inherent damping in both joints and motors. Similar results without requiring the inherent damping has recently appeared in [7].

For flexible beams (and more generally, flexible structures), the importance of passivity has been well recognized, e.g., see [8, 9]. But typically only the set point control is considered and the uniform damping for flexible modes is assumed. There has been also some work involving open-loop, computed torque type of control [10, 11]. We have drawn from this work for the construction of the feedforward trajectory for the error system [3]. A general passive controller design for fully actuated structures has been proposed in [12] which is later applied to a multiple-flexible-link robot in [13]. The portion of our method using naturally passive input/output pairs is similar to that approach, but no inherent damping is required as in [13]. PD stabilization of an undamped flexible beam has been shown in [14]. In [14], PD feedback is also applied to strain gauge feedback which is not passive with respect to the torque input. As expected, only a limited gain margin can be obtained.

The basic structure of our controller consists of a feedforward portion which is driven by the desired trajectory, and a stabilizing feedback which we design based on the consideration of the passivity property of the system (see Fig.1). In this paper, we shall focus only on the design of the feedback portion. The case of naturally passive input/output pairs will be briefly reviewed, but the main goal is to present our recent design experience involving applying passivity based control design to non-passive input/output pairs.

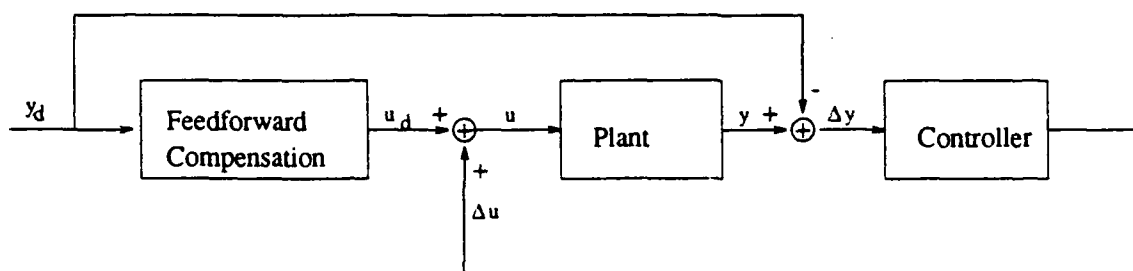


Figure 1: Basic Controller Structure

The basic model considered in this paper is of the following form:

$$M(q)\ddot{q} + C(q, \dot{q})\dot{q} + D(\dot{q}) + F(q) = Bu \quad (1)$$

where M is the mass matrix, C contains terms related to the centrifugal and Coriolis forces, D is the structural damping, F denotes all conservative forces on the system, B is the input matrix, and u is the control input. The Hamiltonian nature of this system implies that M and C satisfy the relationship that $\frac{1}{2}\dot{M} - C$ is skew-symmetric. This implies that the mapping from u to $B^T\dot{q}$ is passive. We shall assume throughout the paper that *collocated displacement and velocity are measurable*. These variables are denoted by

$$y_p \triangleq B^T q \quad y_v \triangleq B^T \dot{q}.$$

In addition to the collocated measurements, we assume some additional non-collocated measurements, $y = h(q, \dot{q})$, are also available. The goal is to design a feedback controller based on both collocated sensors and non-collocated sensors to achieve robust stability and performance. The

non-collocated case will be limited to the linearized system, due to the requirement of an observer. The basic idea is to use the nominal model information to construct a reduced order observer, and then map the reconstructed state to an approximate passive output. A passive feedback filter can then be selected to optimize robustness and performance. The motivation of this approach is that when the model used in the observer is exact, then the same robustness property as in the naturally passive input/output case is obtained. Furthermore, one would expect improved performance, since the loop would be closed in addition to the naturally passive input/output loops. With suitable choice of the observer, passive output map, and the passive feedback filter, one can achieve good robustness and performance even with an inexact model.

The rest of the paper is organized as follows. In Section 2, we consider naturally passive input/output pairs. The main section, Section 3, focuses on the controller design for non-passive input/output pairs. Experimental results involving a single flexible link are presented in Section 4. Section 5 summarizes the paper and presents thoughts on the future work.

2 Passive Input/Output Pairs

For feedback stabilization, we only need to consider the following set point stabilization problem.

Suppose the output of interest is

$$z = C_z q \in \mathbb{R}^m. \quad (2)$$

Choose a feedback control law u based on the measured output, so that $z(t)$ asymptotically converges to the desired output set point z_{des} .

Based on the inherent passivity property of this class of systems, the general procedure described below can be used to construct a solution to the output set point control problem.

1. **Steady State Analysis.** The first step is to find a desired state q_{des} and a feedforward u_{ff} such that

$$C_z q_{des} = z_{des} \quad (3)$$

$$B u_{ff} = F(q_{des}). \quad (4)$$

If these equations are solvable, then the feedforward control can be used to form the error system:

$$M(q)\ddot{q} + D(\dot{q}) + C(q, \dot{q})\dot{q} + F(q) - F(q_{des}) = B u_o$$

where $u_o = u - u_{ff}$.

2. **Error system Stabilization.** Assume that with a static feedback $u_o = -K_p B^T \Delta q + u_1$, the map from u_1 to $B^T \dot{q}$ is passive (this assumption is justified for a number of applications in [15]). Then any strictly passive map from $B^T \dot{q}$ to u_1 , $u_1 = C_v(B^T \dot{q})$ can be used to feedback I/O stabilize the error system. Furthermore, based on an energy Lyapunov analysis, the full state can be shown converging to the largest invariant set on which $B^T \dot{q} = 0$. If the closed loop system is further zero-state detectable (i.e., observable in the case of linear systems) with respect to $B^T \dot{q}$, then the zero error state is asymptotically stable.

In [15], it is shown that for flexible joint robots and flexible beams, $B^T \dot{q}$ is passive but *not* zero-state detectable in the open loop. However, the proportional feedback $B^T \Delta q$ renders $B^T \dot{q}$ zero-state detectable and passive.

The appealing features of the passivity analysis, in the case of naturally passive input/output pairs, can be summarized below:

1. Both linear and nonlinear models for flexible structures can be considered in the same framework of under-actuated Hamiltonian systems with elastic coupling between actuated and un-actuated degrees of freedom.
2. The controller is inherently robust with respect to stability. There is theoretically an infinite gain margin and $(-90^\circ, 90^\circ)$ phase margin.
3. Any passive feedback, C_v , is allowed without affecting stability. Examples have shown that higher order feedback (in contrast to the usual PD control) can lead to significantly improved performance [15].
4. The input/output passivity property is only required over a bandwidth allowing sharp roll off (greater than 20db/decade) of C_v beyond the cut-off frequency.
5. Once a passive feedback filter is chosen, a scalar feedback gain can be adjusted to tune for the best performance without worrying about possible instability (due to the unlimited gain margin).
6. The energy motivated Lyapunov function allows stability analysis of various type of feedforward in the case of output trajectory tracking control. (This aspect is not included in this paper, the full discussion on the tracking problem can be found in [5]).

In our physical experiment (see Section 4 for a more detailed description), there are two sensors that are collocated with the hub torque: a hub potentiometer on the motor shaft and a strain gauge at the base of the beam. The required passive output is the hub angular velocity. This can be obtained in several ways:

1. Direct digital differencing of the potentiometer output and filtering.
2. Analog differentiation of the potentiometer signal.
3. Model based observer to estimate the velocity through the potentiometer (and possibly other sensors).
4. Combination of an accelerometer and potentiometer through some simple filtering.

The first scheme is noisy and adds phase shift which may invalidate the passivity assumption. The second scheme also creates phase distortion and amplifies noise. We have used the third scheme extensively based on a hybrid analytical and identified model (see Section 4 for detail). The performance is satisfactory, but its implementation requires model information and adds more real time computation. Some test has indicated that the last scheme gives a very effective velocity signal. This is the direction we are currently pursuing (more discussion later in this section).

As expected, the hub angle PD feedback maintains stability over a large range of feedback gains (the limiting factors are: sampling effect, distortion of passivity due to sensor/actuator dynamics and nonlinearity, quantization error, sensor/actuator noise, etc.). However, to achieve good performance, in terms of tip displacement, settling time, overshoot, and residue oscillation, the gains must be appropriately chosen. The design method used is simple:

1. Initially ignore the flexible modes and constraint the PD gains so that the rigid body mode alone is critically damped.

2. Restore the flexible modes in the model and adjust the PD gains (subject to the constraint above) to increase the damping ratios of the flexible modes (with particular emphasis on the lowest frequency mode) by using root locus. The root locus analysis also provides an indication of the sensitivity of the closed loop pole locations to the changes in the gains.

As mentioned earlier, currently in our laboratory experiments, an observer is used to construct the hub angular velocity from the estimate of the open loop plant states. In this case, the hub angle velocity signal is unlikely in reality to be positive real (PR) with respect to the plant input torque due to modeling errors, unmodeled non-linearities etc. Digital sampling and A/D quantization further distorts the hub angle velocity estimate. Although the observer provides a significant amount of low pass filtering, the effectiveness is reduced each time the observer pole magnitudes are increased in order to accommodate more plant flexible modes. Hence a direct and accurate hub angle velocity sensor is desirable for the wide bandwidth control of the beam. A further application for such a sensor is the estimation and compensation of hub shaft non-linear friction which limits the small signal performance of the closed loop system.

It is possible to derive the angular velocity signal from an analog hub angle sensor (e.g., a potentiometer) via a bandpass filter which approximates a differentiator at sufficiently low frequencies. However, due to the noise amplification, the bandwidth has to be very limited. An alternative approach is to apply a low pass filter that approximates an integrator at sufficiently high frequencies to an angular acceleration signal and the result is a high frequency velocity sensor. However, the low frequency poles reduces its effectiveness at low frequency. The complementary strengths and drawbacks of these two designs suggest the amalgamation shown in Fig. 2 in which both filters are designed with a common pole and their outputs combined. If s is the Laplace domain variable and ϕ is the hub angle then $s\phi$ is the hub angular velocity and the potentiometer may be modeled as an ideal integrator, while the accelerometer is an ideal differentiator. The combined transfer function is as follows

$$y = \left(\frac{k_1 h_1 \tau s}{s\tau + 1} + \frac{k_2 h_2 s}{s(s\tau + 1)} \right) \dot{\phi} \quad (5)$$

$$= h_1 k_1 \frac{s\tau + \frac{h_2 k_2}{h_1 k_1}}{s\tau + 1} \dot{\phi} \quad (6)$$

If k_1 and k_2 are chosen so that $h_1 k_1 = h_2 k_2$ then $y = h_1 k_1 s \phi$.

This pole/zero cancellation is very robust with respect to errors in the filter gains and simulations that also include non-ideal accelerometer effects such as a resonant peak at 3KHz and a discharge time constant of 16sec and a cross-over filter pole at 1 Hz have a phase distortion of less than $\pm 5^\circ$ over a 500Hz bandwidth. The overall transfer function is shown in Fig. 3.

3 Non-Passive Input/Output Pairs

Controlled structures usually contain more sensors than actuators, due to the weight and cost factors. As a result, the approach described in the previous section can only utilize a subset of the sensors (namely, those that are collocated). Furthermore, some internal subspace may not be strongly observable from just sensors that are collocated with the actuators. It is possible to apply loop transformation to convert the non-positive-real transfer functions from inputs to the non-collocated outputs by adding fictitious feedforwards and compensate for their effects with a feedback loop around the controller. The net result is a relative small feedback gain and reduced gain and phase margins. For our physical experiment, in addition to the hub potentiometer, we have four strain gauges mounted on the beam. The hub angle PD feedback loop provides good

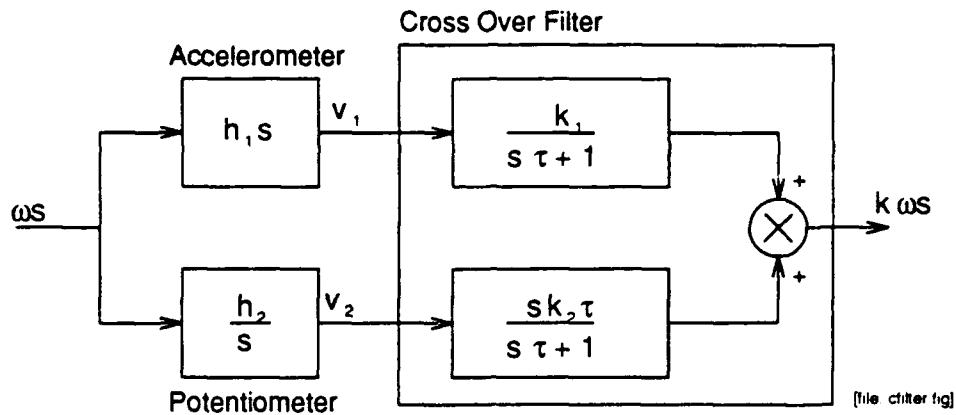


Figure 2: Accelerometer/Potentiometer Velocity Filter

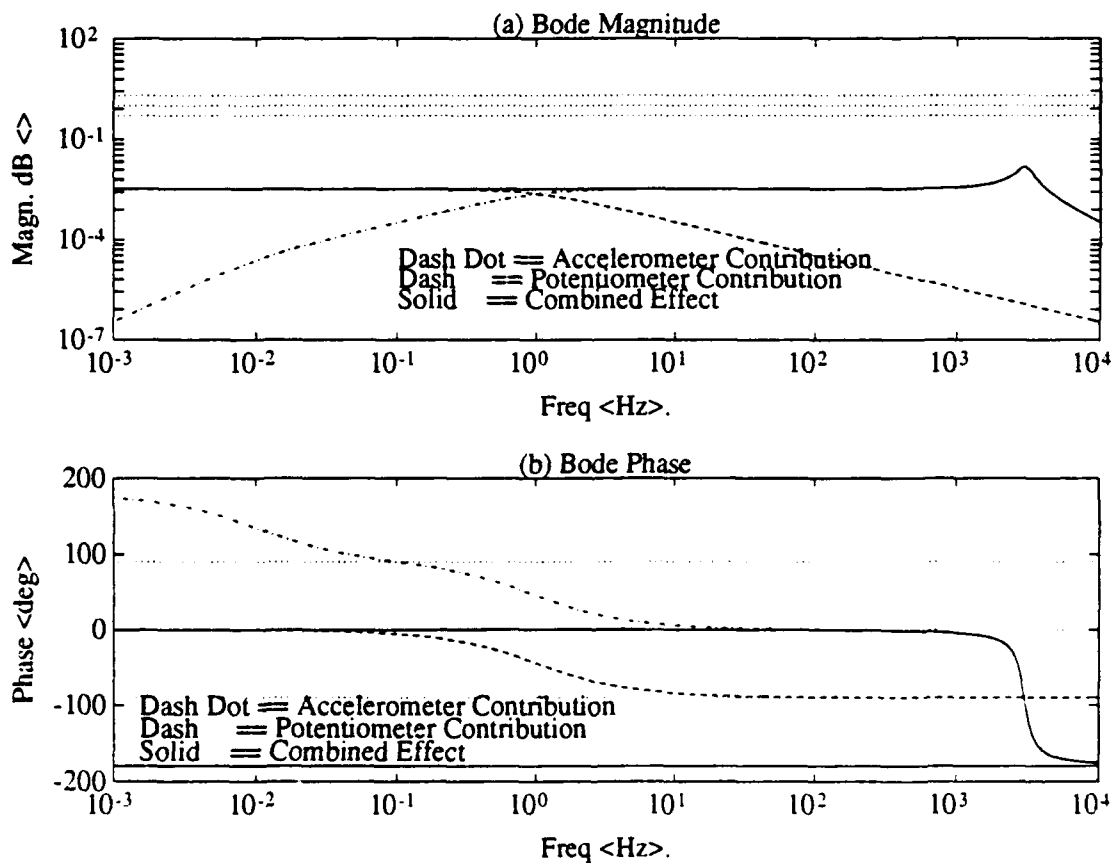


Figure 3: Accelerometer/Potentiometer Velocity Filter Bode Plot

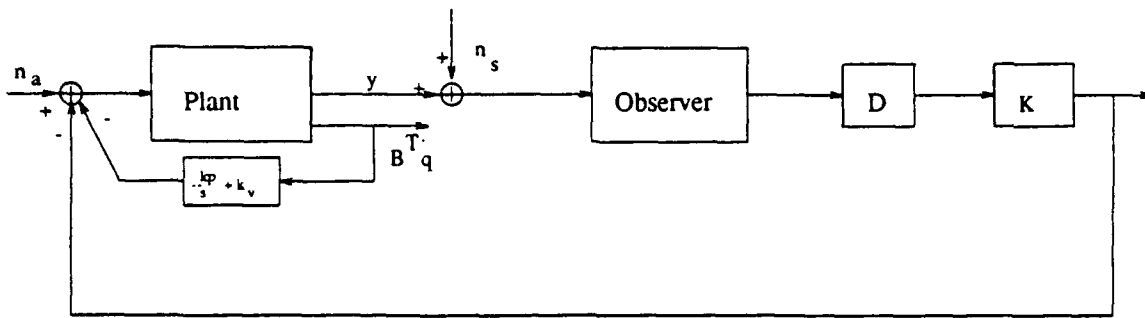


Figure 4: Controller Structure for Synthesized Passive Output Feedback

rigid body mode response with little or no overshoot, approximately critically damps the first flexible mode and offers good gain and phase margins. However, the higher order closed loop flexible modes remain relatively poorly damped. In order to add further damping to these flexible modes, we modify the PD full state feedback gains by closing a second feedback loop around the strain gauges. A direct PD feedback from the strain gauges requires small gains (the third and fourth strain gauges are non-minimum phase with respect to the torque input) and produces little improvement, or even degradation, in terms of closed loop damping over the collocated (hub angle) loop. In this section, we shall present an alternative approach which is based on the observation that there is always some nominal model of the system via either analytic modeling or experimental identification, and it is possible to use this information to “synthesize” an approximately passive output. This approach consists of the following steps:

- Close all naturally passive loops using the procedure described in the previous section
- By using *all* the outputs in an observer, estimate the full state of a reduced order plant with the naturally passive loops closed.
- Synthesize an approximate passive output by passing the estimated full state through an output map D .
- Feedback the approximate passive output to the input through a filter, $K(s)$, which is passive within a bandwidth and rolls off rapidly beyond the cut-off frequency.

The overall block diagram is shown in Fig. 4. The above approach is a direct generalization of the naturally passive case, the only difference being that the passive output here is synthesized using an observer versus a physically available measurement in the previous case.

There are three parameters that need to be selected in this design:

1. Observer feedback gain, L .
2. Passive output map, D , which operates on the reconstructed full state.
3. Passive filter, K , which completes the loop.

We have adopted a procedure to sequentially select these three parameters. The observer gain, L , is chosen based on the consideration of closed loop transient response, actuator and sensor noises, and unmodeled dynamics. After L is selected, the passive output map, D , is chosen based on the

desired modal damping. Finally, the passive filter, K , is chosen to achieve additional robustness and performance.

Observer Feedback Gain

In the ideal case that the plant is exact and the noise can be neglected, the synthesized output, y_{pr} , is related to u by

$$Y_{pr}(s) = D(sI - A_c)^{-1}BU(s) + D(sI - A_L)^{-1}(\hat{x}(0) - x(0))$$

where A_c is the nominal system matrix with the naturally passive loop closed, $A_L \triangleq A_c - LC$, and \hat{x} is the state estimate. Therefore, the first rule is to choose L so that the transient effect of $D(sI - A_L)^{-1}$ is small (i.e., place the poles of A_L beyond the desired closed loop bandwidth).

In a real system, some unmodeled dynamics, ΔP , is always present. For structural systems, if the nominal plant is obtained by direct modal truncation, ΔP will contain at least the higher order modes. Furthermore, the nominal plant parameters are almost always less than exact. With a full state observer, the effect of ΔP on y_{pr} is

$$\Delta Y_{pr}(s) = D(sI - A_L)^{-1}L\Delta P(s). \quad (7)$$

If the actuator noise, n_a , and sensor noise, n_s , are included, the synthesized output becomes

$$Y_{pr}(s) = D(sI - A)^{-1}B(U(s) + N_a(s)) + D(sI - A_L)^{-1}(-BN_a(s) + LN_s(s)) \quad (8)$$

where the first term denotes the output if the true full state were available, and the second term denotes the added contribution due to the noisy signals in the observer. From this discussion, it is clear that the first rule should be moderated so that the bandwidth of $D(sI - A_L)^{-1}L$ should be smaller than the frequency range in which ΔP and n_s are significant (both of these and n_a are usually dominant in the high frequency regime), and the bandwidth of $D(sI - A_L)^{-1}B$ should be smaller than the frequency band of n_a .

As noted in [16], the robustness consideration should be with respect to the true plant input. Suppose the control, u , in the observer is chosen to be $D\hat{x}$ (without the further filtering by K); the observer equation is of the form

$$\dot{\hat{x}} = (A - BD - LC)\hat{x} + Ly \quad (9)$$

The loop gain of interest is then

$$G(s) = D(sI - A + BD + LC)^{-1}LC(sI - A)^{-1}B.$$

If L is chosen based on the Kalman filter technique and the plant is minimum phase, then with the appropriate choice of state noise covariance, $\Sigma = \sigma BB^T$, $G(s)$ approaches $D(sI - A)^{-1}B$ in arbitrary large frequency range provided that σ is sufficiently large. This is the so-called loop transfer recovery (LTR) technique. Note that the actual u may be the filtered version of $D\hat{x}$ even though u in the observer is unfiltered. One problem with LTR is that if there are some stable plant zeros close to the imaginary axis, the observer poles are asymptotically (in σ) attracted to them. This can seriously compromise the overall performance since the closed loop response will be dominated by these weakly damped observer poles.

Passive Output Map

The naturally passive loop can usually provide adequate damping for a number of modes. The non-passive loop should be designed to add damping to other weakly damped modes. To selectively

add damping into specified modes, we choose D based on the Lur'e equations, the solvability of which is a sufficient condition for strict positive realness [17].

$$D = B^T P \quad (10)$$

$$A_c^T P + P A_c = -Q. \quad (11)$$

The weighting matrix Q can be selected to be diagonal with entries corresponding to the desired modes emphasized. If the intercoupling between plant modes due to naturally passive output feedback is small (as is the case for poorly damped flexible modes) then a strong correlation is found between the magnitude of the diagonal elements of Q and the the damping ratios of associated flexible modes when this negative feedback loop is added. This experience is justified in the case ideal case (i.e., perfect model, noise free). Consider the quadratic Lyapunov function candidate

$$V(x) = \frac{1}{2} x^T P x. \quad (12)$$

The closed loop system is governed by (with uncontrollable stable observable dynamics $D(sI - A + LC)^{-1}$ omitted for simplicity of presentation)

$$\dot{x} = A_c x + B u \quad y = D x \quad u = -K y \quad (13)$$

where K , for simplicity, is chosen as a positive definite matrix (K is a positive real filter in general). The time evolution of V along the solution is then given by

$$\dot{V}(x) = -x^T Q x - y^T K y \leq -x^T Q x. \quad (14)$$

Intuitively, if Q is diagonal, then increasing the entries corresponding to certain mode will increase its influence on the rate of decay of $\dot{V}(x)$. More specifically, the exponential decay rate of x is governed by the $Q P^{-1}$. If P is approximately diagonal (as is the case for our experiment), then the entries of Q will have a direct influence on the damping of the corresponding modes.

As mentioned earlier, D also impacts the robustness and noise sensitivity through the transfer function $D(sI - A_L)^{-1} L$ and $D(sI - A_L)^{-1} B$. Ideally, D and L should be selected together, but we do not have a systematic procedure for doing so at this time. At the present, D is chosen based on modal damping consideration. Once D is chosen, L is selected based on other factors described before.

Passive Output Map

In the ideal case, the transfer function from the input to the synthesized output $D\hat{x}$ is a strictly positive real map (with D selected as described above). Then any feedback compensator K that is positive real maintains the closed loop stability. In fact, K only needs to be positive real within the bandwidth of $D(sI - A)^{-1} B$, and can roll off rapidly (faster than 20db per decade) beyond that. This degree freedom can be posed as an optimization problem: find K that is positive real (i.e., K is the stable portion of $K^* + K = M^* M$ for any $M \in \mathcal{RH}_\infty$) such that certain combined robustness and performance criterion is minimized. The optimization criterion may include the following components:

1. Robustness margin: $W_r D(sI - A_L)^{-1} L P (sI - P K)^{-1}$ where $P = D(sI - A_c)^{-1} B$.
2. Tracking performance: $W_t (I + P K)^{-1}$.
3. Disturbance rejection: $W_d (I + P K)^{-1} P$.

Notice that the transfer function $D(sI - A_L)^{-1}L$ occurs in the robustness margin as discussed before in the observer design. The \mathcal{RH}_∞ functions W_r , W_t , and W_d are weighting factors characterizing the unmodeled dynamics, desired trajectory dynamics, and disturbance dynamics, respectively. The optimization problem can then be stated as:

$$\text{minimize} \quad \left\| \begin{bmatrix} W_r D(sI - A_L)^{-1} L P(sI - PK)^{-1} \\ W_t (I + PK)^{-1} \\ W_d (I + PK)^{-1} P \end{bmatrix} \right\|_{H_\infty}$$

over all K that is positive real. This problem can be converted into an H_∞ optimization problem through the following bilinear transformation of K and the nominal plant:

$$\tilde{K} = (I - K)(I + K)^{-1} \quad \tilde{P} = (I - P)(I + P)^{-1}$$

and by using a Lemma in [18]. The detail formulation of this optimization problem can be found in [19].

Currently, the algorithm has been developed for K to be positive real. This can be relaxed outside of the control bandwidth by either cascading additional low pass filters or by modifying the optimization problem through further loop transformation of K and the plant.

Sensor Considerations

To obtain both performance and robustness, it is important to achieve high loop gain in the control bandwidth and small loop gain outside the bandwidth. This can be accomplished by either having fast roll off in the plant or fast roll off in the compensator, K . Roll off in K can be incorporated in the control problem as described above. Shaping of the plant transfer function would require either appropriate placement of sensors or suitable combination of existing sensors, so to maximize the response in the bandwidth of the compensated modes while minimizing that of selected unwanted modes.

In our experiment, the four strain gauges were originally selected simply to avoid zeros of the first four mode shapes. A better strategy would be to place these sensors to maximize the following index:

$$I(x) = \frac{\min\{r_1(x), r_2(x), \dots, r_n(x)\}}{\max\{r_{n+1}(x), \dots, r_{m+n}(x)\}} \quad (15)$$

where n , m are the number of controlled modes and uncontrolled modes, respectively. r_i is the peak associated with the i th mode in the transfer function gain (if there are multiple inputs, the maximum singular value can be used). For strain gauges and a single input, r_i is approximately given by (using the modal frequency, ω_i , as the approximate peak frequency):

$$r_i(x) = \sum_{j=1}^{m+n} \frac{b_j c_j(x)}{((\omega_i^2 - \omega_j^2)^2 + 4\zeta_j^2 \omega_i^2 \omega_j^2)^{\frac{1}{2}}} \quad (16)$$

where b_j is the input coefficient for the i th mode and c_j is proportional to $\psi_j''(x)$, ψ_j being the j th mode shape.

Applying above procedure to our beam model, with $n = 3$ and $m = 2$, results in the optimal strain gauge location at

$$x_1 = .09L \quad x_2 = .325L \quad x_3 = .675L$$

where L is the length of the beam. The plot of the index $I(x)$ as a function of the normalized beam is shown in Fig. 5. The corresponding Bode plots from the actuator input to sensor outputs

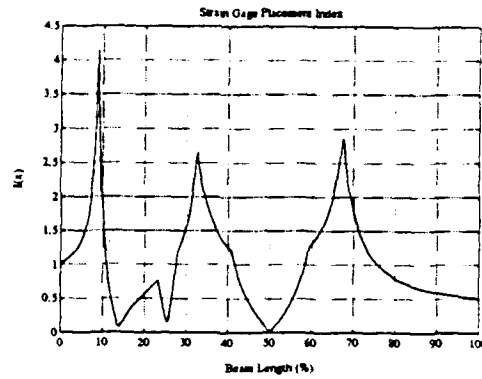


Figure 5: Sensor Placement Optimization Index

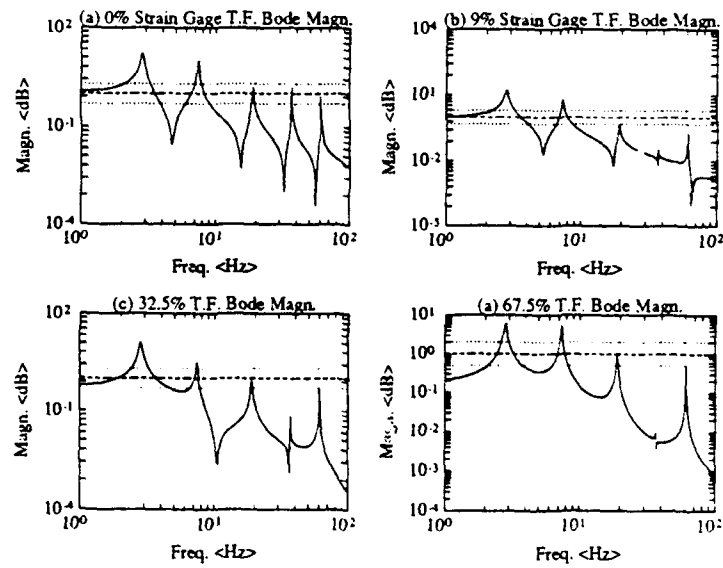


Figure 6: Bode Plots of Optimally Placed Sensors

(including a strain gauge at the hub) are shown in Fig. 6. Compared with the Bode plots of our existing strain gauges shown in the top portion of Fig. 7, the optimally selected ones are preferable in the sense that controlled modes are emphasized over the uncontrolled ones.

Sometimes, the number of controlled modes may not have been chosen a priori, or the sensors may have been chosen based on some other criterion. In this case, the existing sensors can be used to place transmission zeros at one or more unwanted flexible mode frequencies so as to decouple them from the estimated state and hence from the feedback loop. One way to achieve this is to select an appropriate linear combination of the available sensors. Let the new output be y_1 , and

$$y_1 = Hy = HC_N q_N + HC_R q_R \quad (17)$$

where q_N , q_R denote the modeled and residue modal amplitude, and C_N and C_R are the corresponding output matrices. To minimize the effect of the residue modes, we can choose each row of H , h_i , to satisfy $\min_h \frac{\|h_i C_R\|}{\|h_i\|}$. The solution is given by the singular vector that corresponds to the smallest singular value of C_R . With the further requirement that the rows of H should be linearly independent, we can choose the rows of H to be the singular vectors of C_R that corresponds to the r smallest singular values (r is the size of y_1 , which is less than or equal to the number of sensors). If some of the singular values of C_R are too large, r may need to be chosen less than the number of sensors. Once H is chosen, we can further transform the sensors so that C_N is better conditioned. A possible approach is to choose a further output mapping to orthogonalize $(HC_N)^T$:

$$H_1 = \hat{C}_N (HC_N)^T \left((HC_N)(HC_N)^T \right)^{-1} \quad (18)$$

where \hat{C}_N^T is the orthogonalized $(HC_N)^T$. Then choose the new output to be

$$y_1 = \frac{H_1}{\|H_1\|} Hy. \quad (19)$$

For our experimental setup, we combine the four strain gauges into two new outputs while notching out flexible modes #4 and #5. The comparative Bode plots are shown in Fig. 7.

4 Experimental Results

In this section, we will present some experimental results of applying the design procedure described in this paper to a flexible beam rotating in a horizontal plane. There is a single actuator and five sensors, two are physically collocated and three are not, and none is naturally passive with respect to the input. We will first briefly describe the physical facility and the analytical modeling of the system. Then the results related to the following experiments are presented:

1. The Bode plots (from the desired angle to various sensors) and a 45° step response of the following controllers are compared:
 - (a) Hub PD feedback (with an observer synthesized hub velocity). Gains are chosen to critically damp the rigid body mode and the first flexible mode. A Kalman filter is used to reconstruct the hub angular velocity.
 - (b) Hub PD feedback plus an additional synthesized positive real feedback which emphasizes the second and third flexible modes. A reduced order Luenberger observer with poles placed between the third and fourth flexible modes is used. The hub angle and all four strain gauge outputs are fed into the observer.

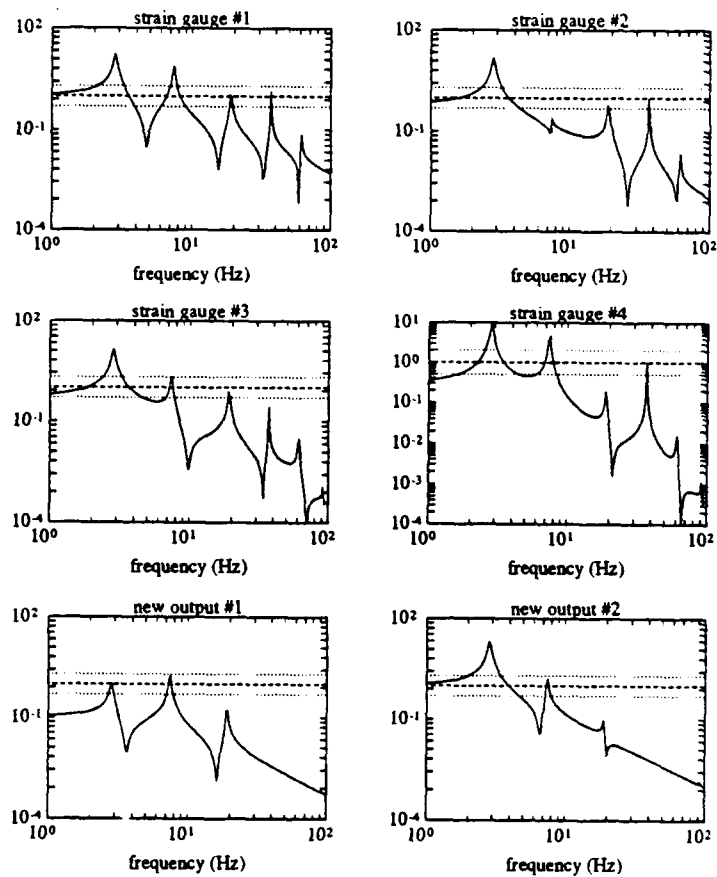


Figure 7: Transfer Function Comparison

- (c) Same as the case above except a Kalman filter (same as in case 1a) is used as the observer. The four strain signals are mapped into two outputs to notch the 4th and 5th mode. These two new outputs together with the hub angle are then used in the observer.

We will see that the last two cases perform as expected: dampings of the second and third flexible modes are significantly increases as compared with the PD feedback alone. The reduced order Luenberger is somewhat easier to design since the poles can be directly placed, and performs better than the Kalman filter. This is possibly due to the relative insensitivity of the observer poles to modeling error in the case of a large number of sensors. When the notching combination is used (reducing the number of outputs to two), the reduced order observer actually results in an unstable design on the physical system.

2. In the ideal case, the gain in the synthesized positive real output feedback loop can be arbitrarily increased. The possibility of using this property to fine tune performance is demonstrated by scaling the gain in the third controller above by 2, 4, and 6, respectively. From the corresponding Bode plots, we will see that higher gains (at least for the scale chosen) result in larger damping.

Description of the Physical Experiment

The single flexible link testbed is depicted in Figure 8. The central component is the flexible beam which is chosen to provide bending in the horizontal plane. Geometric and inertial properties of the beam is shown in Table 1. The beam is driven by a DC motor at one end about a vertical axis in order to excite the flexible modes, and the other end is free. The motor is energized by a power amplifier which is controlled by a single voltage signal; the power amplifier-motor combination provides an approximately linear voltage to beam hub torque relationship. The hub angle is converted to a voltage signal by a potentiometer. Four strain gauges are mounted on the beam, located at $[.0065m, .2715m, .366m, .579m]$ away from the hub. The beam strains at these locations are converted to voltage signals by strain gauges. The real time computer is a networked set of four Inmos Transputer micro-processors which are connected to a 486PC host for software development and user interface. These Transputers also connect to a VME signal bus on which reside the digital to analog (D/A) and analog to digital (A/D) circuit cards providing the motor drive (computer output) and sensor (computer input) signal interfaces. The control analysis and design on performed on SUN Sparcstations using MATLAB. The controller parameters are saved in a MATLAB file which are then read in by the real time computer. The sensory data are also saved in a MATLAB file after each experiment. A picture of the physical laboratory is shown in Fig. 9.

Parameter	Symbol	Units	Value
Width	w	m	$1.5875e-3$
Height	h	m	$1.03e-1$
Length	l	m	1.098
Density	ρ	Kg/m^3	$2.713e3$
Youngs Modulus	E	Kg/m^2	$6.895e10$

Table 1: Aluminum Beam Material Parameters

Dynamic Model

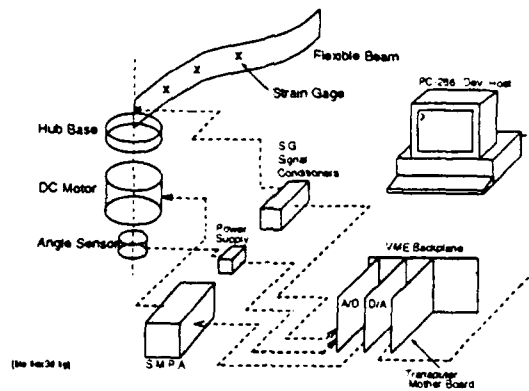


Figure 8: Flexible Beam Testbed

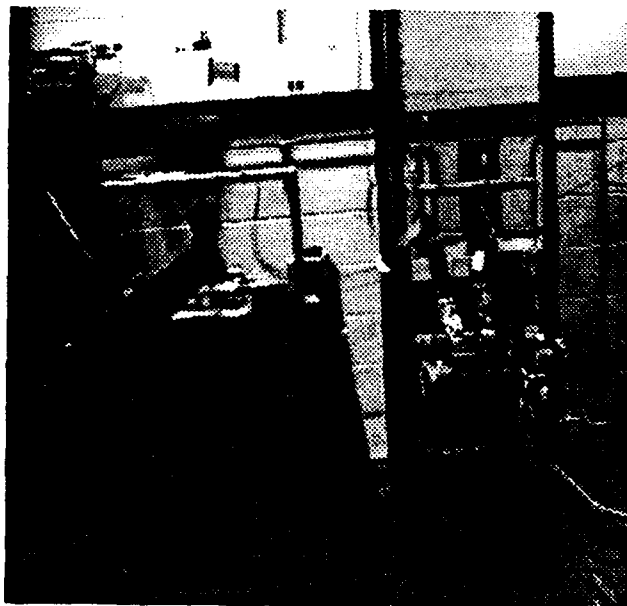


Figure 9: Flexible Beam Physical Facility

i	f_i Hz	\hat{f}_i Hz	$\frac{100(f_i - \hat{f}_i)}{f_i}$	$b_i \frac{1}{Nm}$	$\hat{\zeta}_i$
0	0	0		3.19	
1	2.83	2.83	0.0	7.65	0.0229
2	7.42	7.15	3.8	4.22	0.0115
3	19.06	17.8	7.1	1.53	0.0097
4	36.99	35.4	4.5	0.768	0.0025
5	61.03	58.0	5.2	0.462	0.0016
6	91.10	90.8	0.3	0.309	0.0024
7	127.21	126.3	0.7	0.221	
8	169.34	166.6	1.6	0.166	
9	217.50	214.4	1.4	0.129	

Table 2: Beam Normal Mode Parameters

The linearized model is given by [20]

$$EI_a \frac{\delta^4 v}{\delta x^4} + \rho_x \frac{\delta^2 v}{\delta t^2} = 0 \quad (20)$$

$$\tau - I_H \ddot{\phi} + EI_a v''(0, t) = 0 \quad (21)$$

with the boundary conditions

$$v(0, t) = 0, \quad v'(0, t) = \phi, \quad v''(0, t) = 0, \quad v'''(L, t) = 0$$

where ϕ is the hub angle. This model is spatially discretized using the natural mode shapes, resulting in an infinite set of ordinary differential equations [20]. The analytic modal frequencies are very closely matched with the experimentally identified frequencies, up to the ninth flexible mode (see Table 2). The damping is obtained experimentally.

Control Experiments: PD vs. PD + filtered strains

The hub torque and hub angular velocity form naturally passive pairs. However, only the hub angle is available. Hence, the reconstructed velocity from the observer is used to close the collocated loop. For the result shown here, a Kalman filter is used (with a processed output to notch out the 4th and 5th flexible modes). Based on the root locus of the first two modes (rigid body and the first flexible mode), the PD gains are chosen to be

$$K_p = 2.472 \quad K_v = 1.287.$$

This controller performs fairly well in both simulation and experiment. Based on a hybrid analytical/experimental model (identified damping, but analytical modal frequencies and mode shape), hub PD feedback (with observer and unmodeled dynamics included in the simulation) substantially increases the damping on the rigid body mode and the first two flexible modes. The specific values are tabulated in Table 3.

For the strain gauge loop, various observer design techniques were used. With the five available sensors, the reduced order pole placement observer design (where poles are placed between the third and the fourth flexible modes) performs the best. With the same controller but a Kalman filter designed using the LTR technique, the performance is very poor. This is due to the weakly damped observer poles caused by the weakly damped plant zeros. With the hub PD feedback, the

Mode #	f_{ol}	f_{pd}	f_{pr}	ζ_{ol}	ζ_{pd}	ζ_{pr}	τ_{ol}	τ_{pd}	τ_{pr}
0							0.92	0.38	0.40
1	2.83	1.10	1.06	0.0229	0.81	0.77	2.5	0.18	0.19
2	7.15	6.77	6.71	0.0115	0.066	0.133	1.9	0.35	0.18
3	17.8	17.8	17.7	0.0097	0.0143	0.029	0.87	0.63	0.31
4	35.4	35.4	35.2	0.0025	0.0032	0.0026	1.7	1.41	1.74
5	58.0	58.0	57.9	0.0016	0.0017	0.0013	1.6	1.62	2.12

1. subscript ol \Rightarrow open loop plant parameter,
- subscript pd \Rightarrow PD compensated system parameter,
- subscript pr \Rightarrow PD + PR compensated system parameter.
2. $\tau_{xx} = \frac{1}{2\pi f_{xx}\zeta_{xx}}$

Table 3: Compensator Pole Parameters

dominant zeros associated with the hub angle and the strain gauges, are located at $-0.5 \pm 6.7j$, $-0.4 \pm 30j$, $-0.5 \pm 46j$, $-0.6 \pm 61j$, $-1.2 \pm 133.2j$, respectively. When the state noise covariance is chosen to be

$$\Sigma_x = 5 * \text{diag}\{0, 100, 0, 1, 0, 1, 0, 1\}$$

the closed loop performance is adequate. However, the experimental gain margin is substantially improved when the four strain gauges are combined to produce two outputs which block flexible modes 4 and 5. However, the reduced number of output performs poorly with the pole placement type observer. This is possibly due to the fact that the pole placement algorithm in MATLAB minimizes the gain sensitivity when a large number of feedback channels are available. This would lead to the enhanced robustness with respect to the modeling error. The frequency and damping comparison based on the simulated plant is shown in Table 3. The experimental Bode plots (of strain gauges #1, the one closest to the hub, and #4, the one closest to the tip) and step responses are shown in Fig. 10–Fig. 12.

The Bode plots are obtained by using Shroeder-phased multiple sinusoids (as discussed in [21]) feeding in the desired hub angle. It is seen that the damping of the rigid body and first flexible mode are very close in all three cases; this is deliberately chosen as we have designed the non-collocated loop to emphasize the next two flexible modes. And indeed, the dampings on these two modes are increased as compared to the PD feedback. The peak amplitude of each mode is roughly inversely proportional to the damping of that mode. The experimental damping improvement roughly corresponds to the predicted values in the simulation. Around the fifth flexible mode (about 60Hz), there is an additional unmodeled mode. This may be due to an unmodeled mode of the table support.

The step response also shows less transient oscillation with the synthesized positive real output feedback. Between the two types of observers, the reduced order Luenberger appears to perform better. However, the comparison between the two is not meant to be a conclusive and quantitative one. Each offers some design advantages and drawbacks, and, more importantly, both can substantially increase the performance over the PD loop alone.

Feedback Loop Scaling

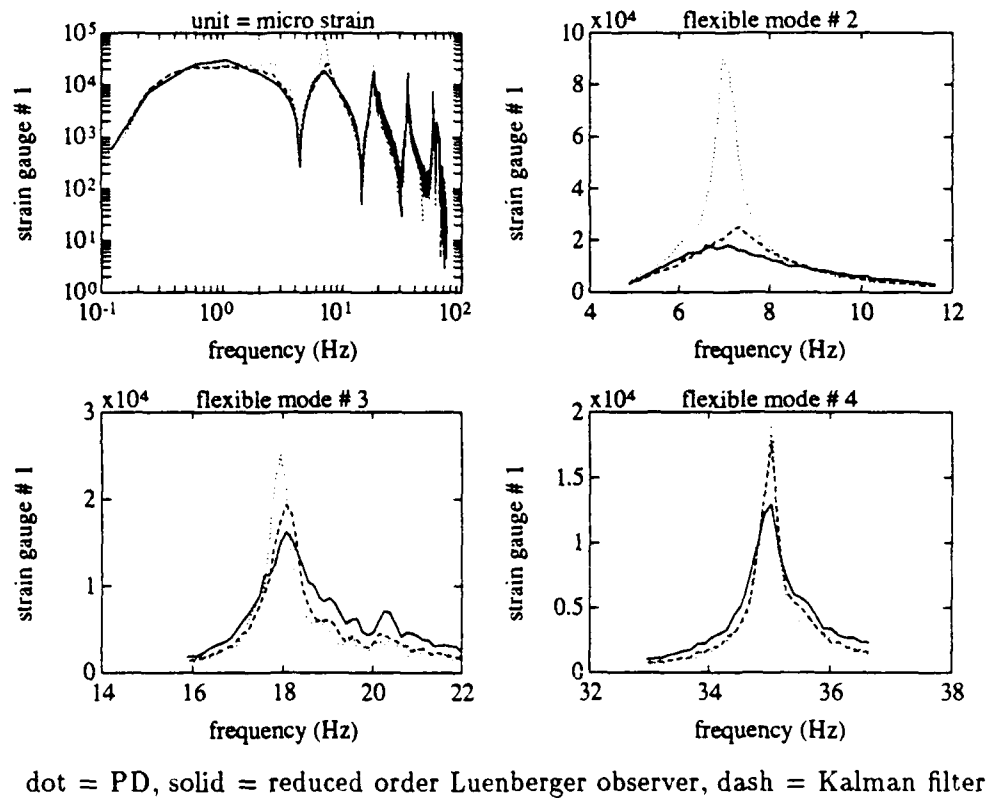


Figure 10: Experimental Bode Plots, Strain Gauge # 1

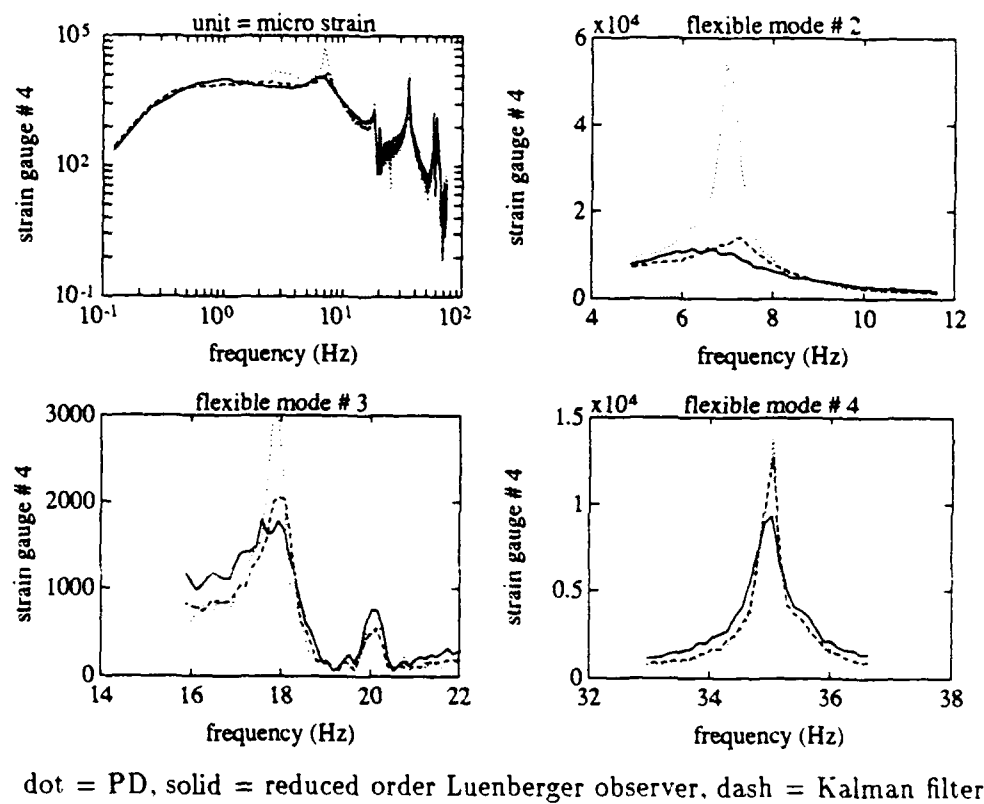
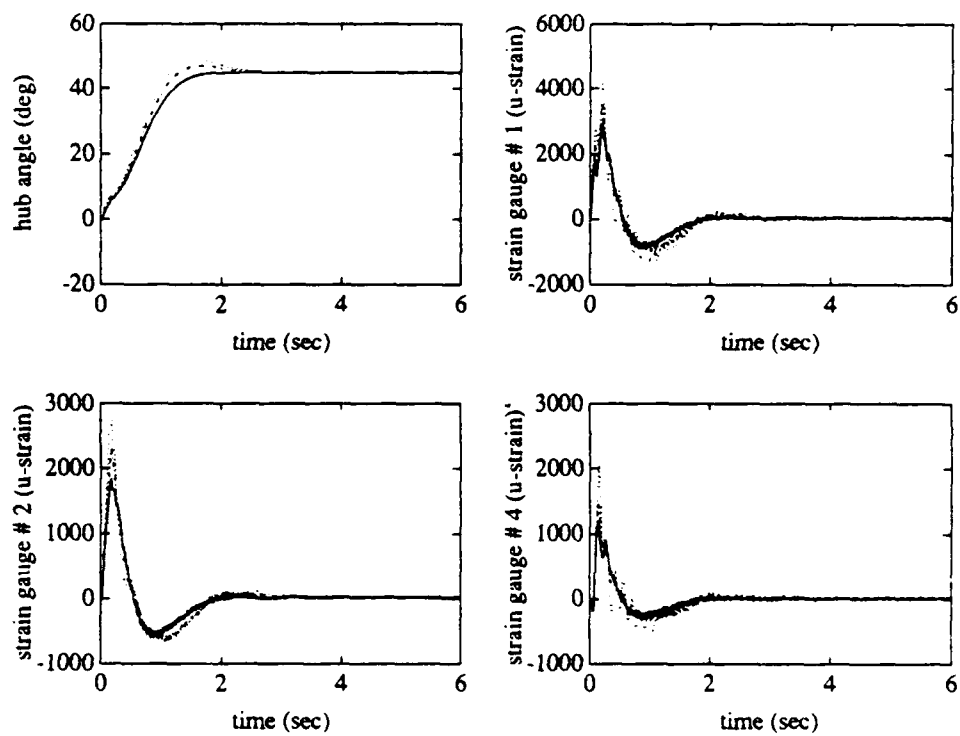


Figure 11: Experimental Bode Plots, Strain Gauge # 4



dot = PD, solid = reduced order Luenberger observer, dashdot = Kalman filter

Figure 12: Step Response Experimental Results

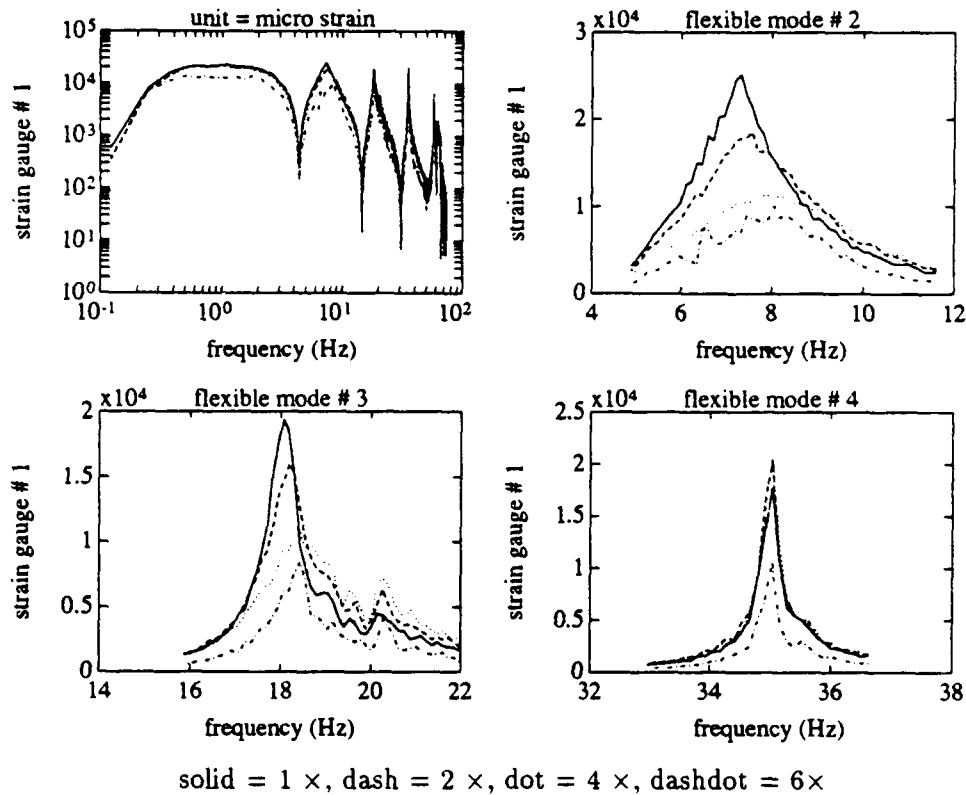


Figure 13: Experimental Bode Plots, Strain Gauge # 1

One feature of passive feedback is the theoretical infinite gain margin. This degree of freedom in the feedback gain scaling offers a convenient scalar tuning parameter for performance. We take the Kalman filter based controller in the previous part and scale the loop gain in the synthesized passive loop (i.e., scaling D by a constant) by 2, 4, and 6, respectively. The resulting Bode plots (of strain gauges # 1 and # 4) of all four cases are shown in Fig. 13–14. It is seen that the damping of all flexible modes monotonically increases with higher scaling. This is certainly not always guaranteed, but it does illustrate the advantage of having this performance tuning parameter available without needing to be overly concerned of its impact on stability.

There are two additional observation we made based on our experience:

1. When the Kalman filter does not have a sharp roll off, the physical experiment becomes unstable. This demonstrates the importance of shaping $D(sI - A_L)^{-1}L$ in relation to the unmodeled dynamics in the observer.
2. The sensor combination to notch out unwanted modes is pivotal in the Kalman filter design. Without it, much lower gain (i.e., smaller Q in the Lyapunov Equation) needs to be used to ensure stability. An alternative is to build a larger observer to include some of the uncontrolled modes and not use them in the controller feedback.

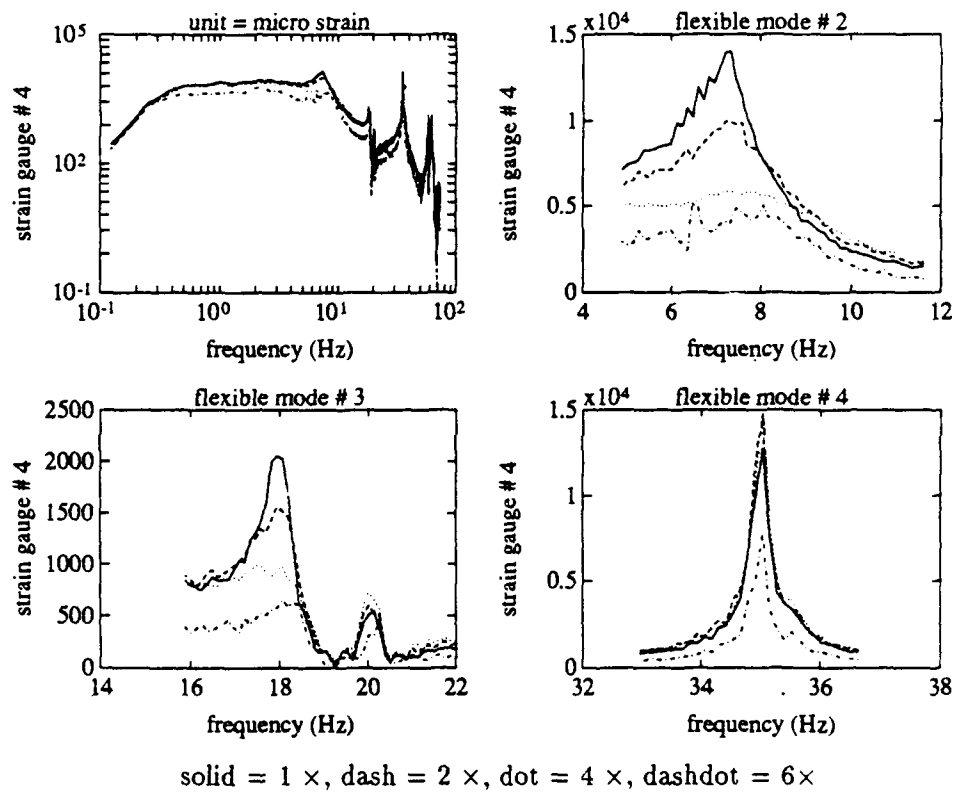


Figure 14: Experimental Bode Plots, Strain Gauge # 4

5 Conclusion and Future Work

Stabilization of flexible structures with naturally passive input/output pairs have been extensively studied in the past. For non-passive pairs, direct negative feedback requires small gain and has severely limited gain and phase margins. This paper presents an observer based extension of the passive controller design to the case of non-passive input/output pairs. The selection of three key parameters: observer gain, L , passive output map, D , and passive filter, K , are discussed based on the performance, robustness, and noise sensitivity considerations. Simulation and experimental results have demonstrated the basic viability of this method. However, some fundamental issues remain. Based on our experience thus far, we have identified the following areas for further research:

1. Systematic design of L in the observer to shape $D(sI - A_L)^{-1}L$ which affects the noise sensitivity and robustness with respect to the unmodeled dynamics.
2. Further investigation of the optimization of the passive compensator $K(s)$.
3. Extension to the multiple articulated bodies where the issue of nonlinear observer design needs to be addressed.

Acknowledgment

This work was supported in part by the National Science Foundation under Grant No.MSS-9113633 and Army Research Office under grant DAALO3-92-G-0123

References

- [1] L. Meirovitch. *Analytic Methods in Vibration*. The MacMillan Company, New York, 1967.
- [2] M. Takegaki and S. Arimoto. A new feedback method for dynamic control of manipulators. *ASME J. Dynamic Systems, Measurement and Control*, 102, June 1981.
- [3] L. Lanari and J.T. Wen. A family of asymptotic stable control laws for flexible robots based on a passivity approach. CIRSSSE Report 85, Rensselaer Polytechnic Institute, February 1991.
- [4] M.W. Spong. Control of flexible joint robots: A survey. UILU-ENG-90-2203 DC-116, University of Illinois at Urbana-Champaign, February 1990.
- [5] P. Sicard, J.T. Wen, and L. Lanari. Trajectory tracking of flexible joint manipulators with passivity based controller. Internal report, Rensselaer Polytechnic Institute, August 1992.
- [6] S. Arimoto and F. Miyazaki. Stability and robustness of PD feedback control with gravity compensation for robot manipulator. In *ASME Winter Meeting*, pages 67-72. Anaheim, CA. December 1986.
- [7] P. Tomei. Point-to-point control of elastic joint robots. In *Proc. Int. Symp. on Intelligent Robotics*. Bangalore, India, January 1991.
- [8] R.J. Benhabib, R.P. Iwens, and R.L. Jackson. Stability of distributed control for large flexible structures using positivity concepts. In *AIAA Guidance and Control Conference, Paper No. 79-1780*, Boulder, Co., August 1979.
- [9] J.-N. Juang and M. Phan. Robust controller designs for second-order dynamic systems: A virtual passive approach. Nasa tm-102666, NASA Langley, May 1990.

- [10] E. Bayo. Computed torque for the position control of open-chain flexible robots. In *Proc. 1988 IEEE Robotics and Automation Conference*, pages 316-321, Philadelphia, PA, April 1988.
- [11] D.S. Kwon and W.J. Book. An inverse dynamic method yielding flexible manipulator state trajectories. In *Proc. 1990 American Control Conference*, pages 186-193, San Diego, CA, May 1990.
- [12] B. Paden and B. Riedle. A positive-real modification of a class of nonlinear controllers for robot manipulators. In *Proc. 1988 American Control Conference*, Atlanta, GA, June 1988.
- [13] B. Paden, B. Riedle, and E. Bayo. Exponentially stable tracking control for multi-joint flexible-link manipulators. In *Proc. 1990 American Control Conference*, pages 680-684, San Diego, CA, June 1990.
- [14] H.G. Lee, H. Kanoh, S. Kawamura, F. Miyazaki, and S. Arimoto. Stability analysis of a one-link flexible arm control by a linear feedback law. In S.G. Tzafestas T. Futagami and Y. Sunahara, editors, *Distributed Parameter Systems: Modelling and Simulation*, pages 345-352. Elsevier Science Publishers B.V. (North-Holland), 1989.
- [15] L. Lanari and J.T. Wen. Asymptotically stable set point control laws for flexible robots. *to appear in System and Control Letters*, 1992.
- [16] J.C. Doyle and G. Stein. Multivariable feedback design: Concepts for a classical/modern synthesis. *IEEE Transactions on Automatic Control*, 26:4-16, 1981.
- [17] J.T. Wen. Time domain and frequency domain conditions for strict positive realness. *IEEE Trans. on Automatic Control*, 33(10), Oct 1988.
- [18] K. Glover and J.C. Doyle. State space formulae for all stabilizing controllers that satisfy an h_∞ norm bound and relations to risk sensitivity. *Systems and Control Letters*, 11:167-172, 1988.
- [19] X. Chen. Stability analysis and controller synthesis of distributed parameter systems with unbounded input and output operators. Internal report, Rensselaer Polytechnic Institute, April 1992.
- [20] F. Wang and J.T. Wen. Nonlinear dynamical model and control for a flexible beam. CIRSSE Report 75, Rensselaer Polytechnic Institute, November 1990.
- [21] D. Bayard. Statistical plant set estimation using Schroeder-phased multisinusoidal input design. In *Proc. 1992 American Control Conference*, pages 2988-2995, Chicago, IL, 1992.